



**Azole-based compounds as potential anti-acanthamoeba agents**

Journal:	<i>RSC Medicinal Chemistry</i>
Manuscript ID	MD-RES-01-2024-000029.R1
Article Type:	Research Article
Date Submitted by the Author:	15-Feb-2024
Complete List of Authors:	Qubais-Saeed, Balsam ; University of Sharjah Hamdy, Rania; University of Sharjah Akbar, Noor; University of Sharjah Khan, Naveed Ahmed ; Istinye Universitesi Soliman, Sameh; University of Sharjah,

SCHOLARONE™  
Manuscripts

**Azole-based compounds as potential anti-acanthamoeba agents**

Balsam Qubais Saeed<sup>1,2</sup>, Rania Hamdy<sup>1,3,4</sup>, Noor Akbar<sup>1,2</sup>, Naveed Ahmed Khan<sup>5</sup>, Sameh S.M. Soliman<sup>1,6\*</sup>

<sup>1</sup> Research Institute of Medical and Health Sciences, University of Sharjah, Sharjah, 27272, UAE.

<sup>2</sup> Department of Clinical Sciences, College of Medicine, University of Sharjah, Sharjah, 27272, UAE.

<sup>3</sup> Research Institute for Science and Engineering (RISE), University of Sharjah, Sharjah, 27272, UAE.

<sup>4</sup> Faculty of Pharmacy, Zagazig University, Zagazig 44519, Egypt.

<sup>5</sup> Microbiota Research Centre, Istinye University, Istanbul, 34010, Turkey.

<sup>6</sup> College of Pharmacy, University of Sharjah, Sharjah P.O. Box 27272, UAE.

**\*Corresponding address**

Sameh S.M. Soliman, Department of Medicinal Chemistry, College of Pharmacy, University of Sharjah, Sharjah, UAE, Tel: +97165057472, Email: [ssoliman@sharjah.ac.ae](mailto:ssoliman@sharjah.ac.ae)

## Abstract

*Acanthamoeba castellanii* is an opportunistic pathogen with public health implications, largely due to its invasive nature and non-specific symptoms. Our study focuses on the potential of azole compounds, particularly those with triazole scaffolds, as anti-amoebic agents. Out of 10 compounds, compounds **T1** and **T8** exhibited effective anti-*Acanthamoeba* activity with MIC<sub>50</sub> values of 125.37 and 143.92 µg/mL, respectively. Interestingly, compounds **T1**, **T4**, **T5** and **T8** revealed the profound anti-excystation activity with MIC<sub>50</sub> at 32.01, 85.53, 19.54 and 80.57 µg/mL, respectively, alongside limited cytotoxicity to human cells. The study underscores the potential of **T1**, **T4**, **T5**, and **T8**, thiazole-based compounds, as anti-*Acanthamoeba* agents by both eliminating amoeba viability and preventing excystation, via preserving the amoeba in its latent cyst form, exposing them to elimination by the immune system. Notably, compounds **T1**, **T4**, **T5**, and **T8** showed optimal molecular properties, moderate oral bioavailability, and stable complex formation with *Acanthamoeba* CYP51. They also display superior binding interactions. Further research is needed to understand their mechanisms and optimize their efficacy against *Acanthamoeba* infections.

**Keywords:** *Acanthamoeba castellanii*; Azole; anti-amoebic agents; Excystation

## Introduction

*Acanthamoeba castellanii* is an opportunistic pathogenic free-living amoeba primarily accountable for severe condition as fatal granulomatous amoebic encephalitis (GAE) and blinding keratitis called *Acanthamoeba keratitis* (AK) <sup>1-3</sup>. *Acanthamoeba* is ubiquitous in various natural environments, from soil to water bodies, including lakes, rivers, and artificial ecosystems like swimming pools and water systems <sup>4-6</sup>. In general, the parasite enters the body via respiratory system by inhaling contaminated soil or breathing in polluted water. The amoeba invades the bloodstream, spreads systemically and eventually crosses the blood-brain barrier to reach the brain <sup>2,7</sup>. Its ability to invade the central nervous system (CNS) results in tissue damage, making diagnosis challenging due to its non-specific clinical presentation and radiological characteristics <sup>2</sup>. The lack of available understanding of amoeba's intricate pathogenesis challenges the development of anti-amoebic treatment <sup>8</sup>. Considering the challenges posed by *Acanthamoeba castellanii*, there is an urgent and compelling need for the discovery and development of novel anti-amoebic agents. Azole drugs have been implied for their antimicrobial, antiparasitic, and antibacterial activities <sup>9</sup>. Azole, particularly imidazole, oxadiazoles, triazoles, and thiadiazols, is a highly functionalized scaffold with a vital role in the design of anti-amoebic drugs <sup>10</sup>. Azoles are antifungal drugs that disrupt the cell membrane by inhibiting 14- $\alpha$  demethylase lanosterol. 14- $\alpha$  Demethylase lanosterol is also a key enzyme in *Acanthamoeba's* sterol biosynthesis. Sterols are one of the most important lipids in the eukaryotic cell membrane, performing important structural and signalling function <sup>11</sup>.

Azole drugs such as nitroimidazoles have been among the most important drugs in fighting amoebiasis <sup>12</sup>. Metronidazole is a drug of choice for amoebiasis treatment, however under anaerobic condition the nitro group is converted to cytotoxic nitroso radical inside the cell that binds non-specifically to the DNA and enzymes <sup>13</sup>. As a negative consequence, it causes

toxicity alongside evolved resistance to the bacteria and protozoa <sup>14</sup>. Anti-amoebic activities of azole drugs against free-living amoebae indicated that, hybrid structure of metronidazole with triazole scaffold showed improved potency <sup>12</sup>. Additionally benzimidazole is more effective than metronidazole against *E. histolytica* <sup>15</sup>, and voriconazole showed potent activity against *Acanthamoeba* trophic stages <sup>16</sup>. This highlights the relevance of triazole scaffold in the design and development of novel effective anti-amoebic medications. Therefore, we aim to utilise the efficacy of azole-containing drugs, like metronidazole, to treat amoebiasis. However, to address the toxicity and cross-resistance issues by metronidazole and to enhance the effectiveness, triazole scaffolds that don't have nitro groups were introduced.

## Results

### *Rational design*

The relevance of imidazole scaffold containing drugs such as metronidazole, tinidazole and ornidazole (**Figure 1**) in amoebiasis treatment provides a platform for drug design and development. However, the accompanied toxicity and emergence of cross resistance drive the need to discover and develop other candidates with enhanced efficacy, physiochemical characteristics, and safety profiles. Here, the introduction of triazole scaffold as metal binding group that can inhibit the ergosterol biosynthesis was used to design anti-amoebic candidates without nitro group to overcome toxicity (**Figure 2**).

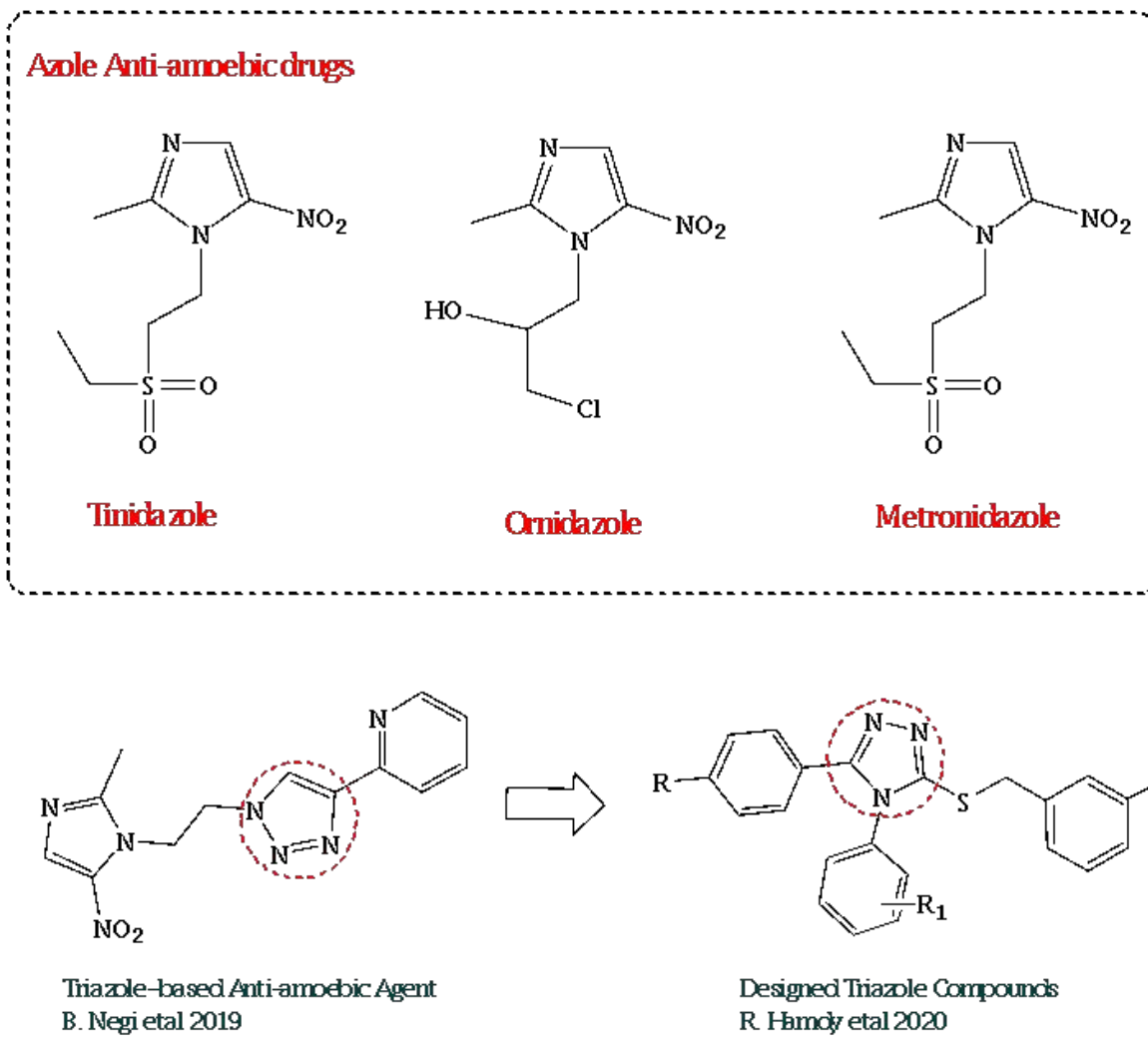


**Figure 1.** Rational design of azole based anti-amoebic agent.

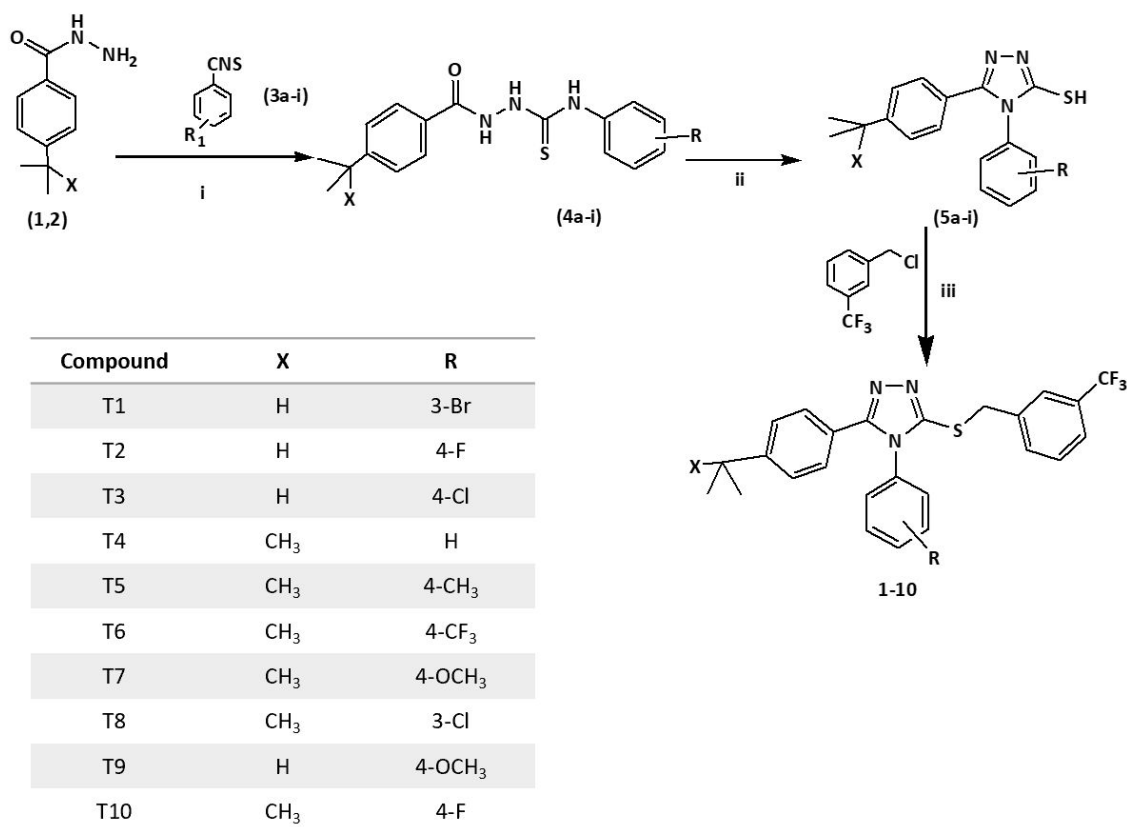


**Figure 2.** Synthetic scheme of azole compounds. Reagent and condition. **i)** ethanol/reflux 3 h; **ii)** 2N NaOH/reflux for 3 h; **iii)** KOH-ethanol-12 h/stirring.

### *Selected azole-designed compounds showed antiamoebic effects against A. castellanii*

The antiamoebic activity of compounds (**T1-T10**) were assessed using amoebicidal assays. The results from the amoebicidal assays revealed that compounds affected the viability of amoeba significantly at 100 µg/mL concentration when compared to negative control (**Figure 3**). Among all the compounds tested **T1**, **T4**, **T5** and **T8** revealed significant amoebicidal properties (**Figure 3**) with 34%, 17%, 27% and 25% reduction in amoebae viability, respectively (**Figure 3**). These compounds were selected for further half minimal inhibitory concentration MIC<sub>50</sub> calculation. MIC<sub>50</sub> analysis revealed that compound **T1** was the most effective among all the compounds showed lower MIC<sub>50</sub> value of 125.37 µg/mL (**Figure 4**). Compounds **T4**, **T5** and **T8** demonstrated higher MIC<sub>50</sub> values of 239.35, 179.57 and 143.92 µg/mL, respectively (**Figure 4**).

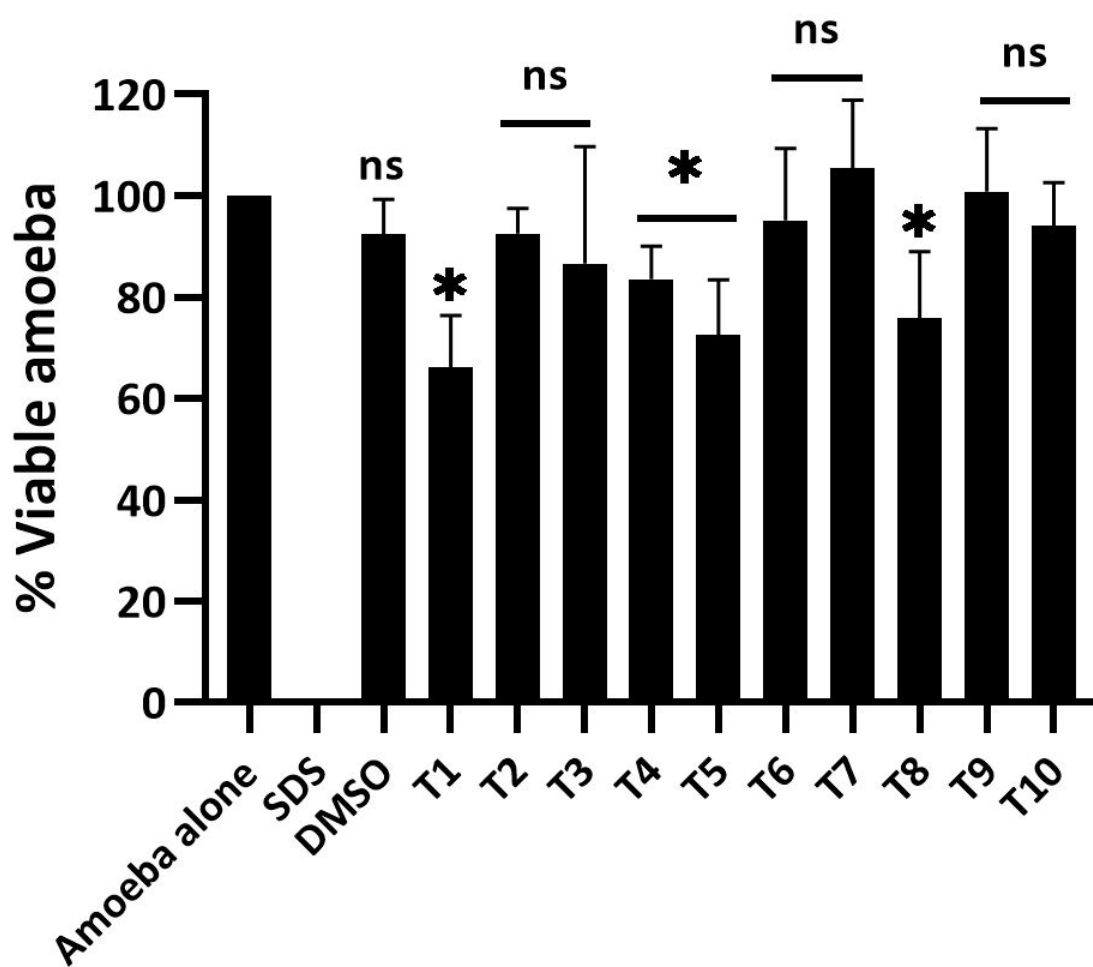


**Figure 3.** Amoebicidal properties of compounds against *A. castellanii*. The compounds exhibit significant amoebicidal activity. All the experiments were performed three time in duplicates and the data presented is the mean  $\pm$  standard error of three independent trails performed in duplicates.

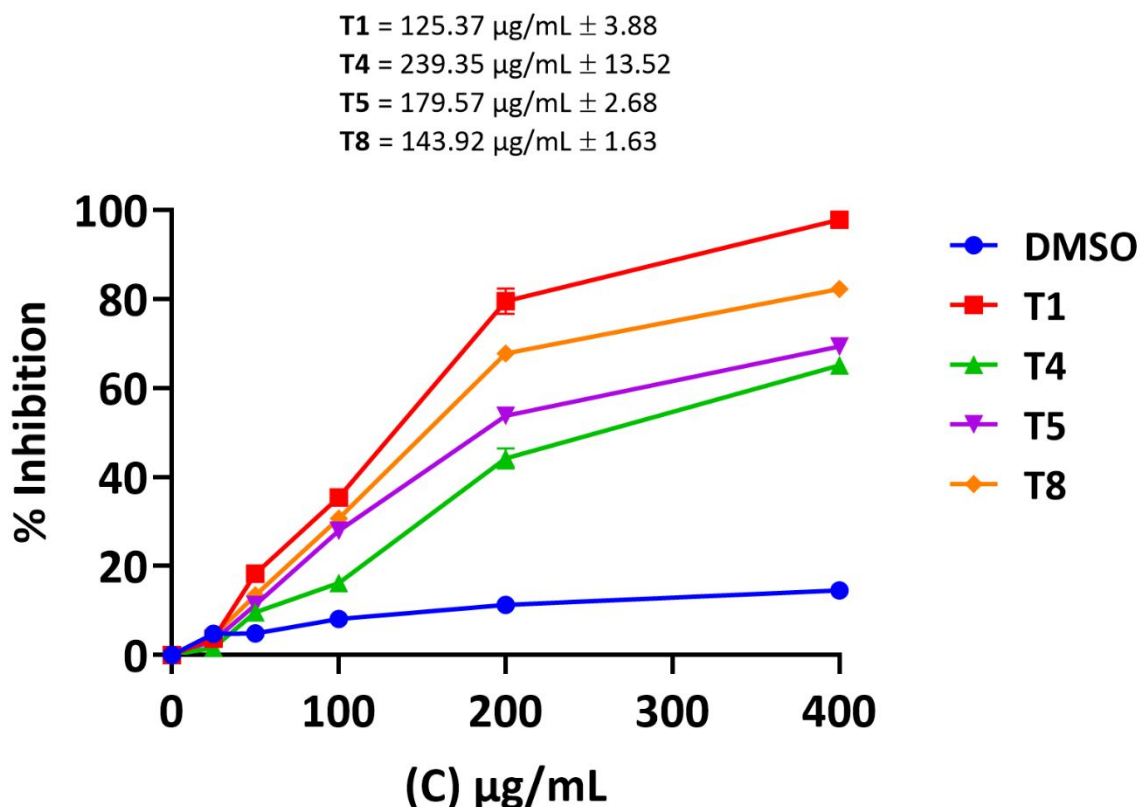


**Figure 4.** Determination of minimum inhibitory concentration of selected compounds against *A. castellanii*. All the experiments were performed three time in duplicates and the data expressed the mean  $\pm$  standard error of three independent experiments done in duplicates.

#### *Compounds did not show encystation but exhibit excystation inhibitory effects*

When these compounds were tested for their encystation properties, none of the compounds showed encystment effects (**Figure 5**). The results from excystation assays showed that all the tested compounds significantly blocked the excystation at 100  $\mu\text{g}/\text{mL}$  concentration ( $P \leq 0.05$ ) (**Figure 6A**). At 100  $\mu\text{g}/\text{mL}$ , **T1**, **T4**, **T5**, and **T8** blocked 77%, 78%, 86% and 78% *A. castellanii* excystation, respectively (**Figure 6A**). Additionally, findings from  $\text{MIC}_{50}$  have shown that compound **T5** exhibited the strongest anti-excystation capability showing half-minimal inhibitory effects at 19.54  $\mu\text{g}/\text{mL}$  (**Figure 6B**). Compound **T1** had relative strong effects demonstrated  $\text{MIC}_{50}$  at 32.01  $\mu\text{g}/\text{mL}$  (**Figure 6B**). On the other hand, compounds **T4** and **T8** showed higher  $\text{MIC}_{50}$  values of 85.53 and 80.57  $\mu\text{g}/\text{mL}$ , respectively (**Figure 6B**).

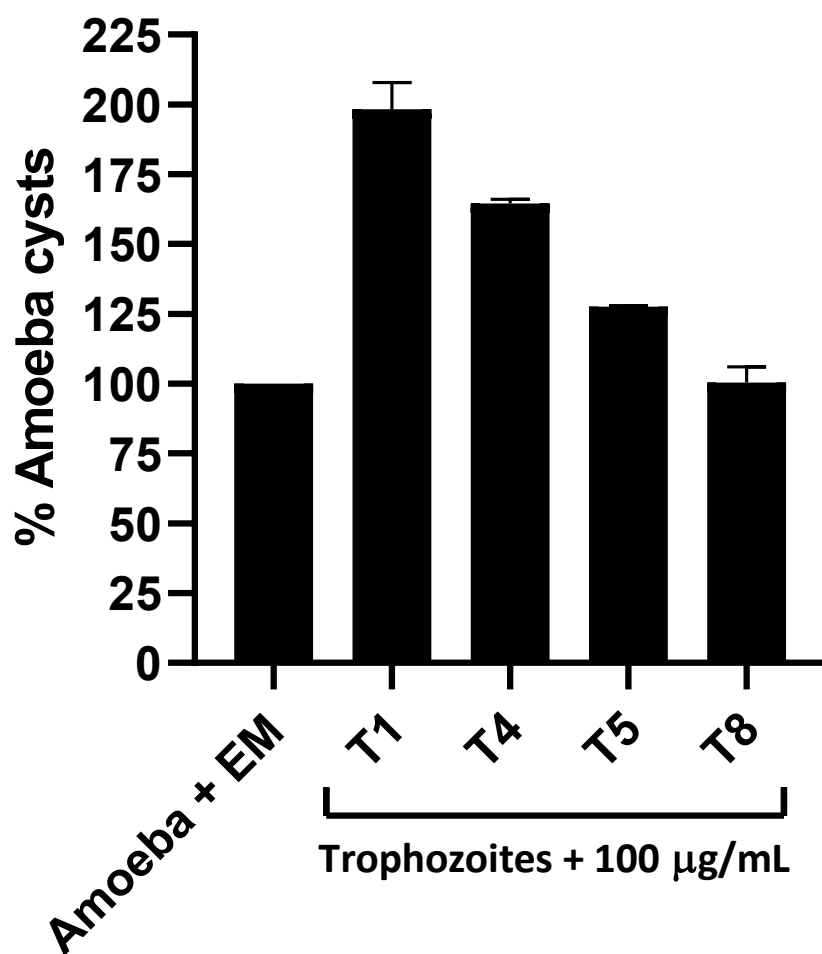


**Figure 5.** Encystation effects of compounds against *A. castellanii* trophozoites. All the experiments were performed three time in duplicates and the data presented the mean  $\pm$  standard error of three autonomous assessments performed in duplicates.

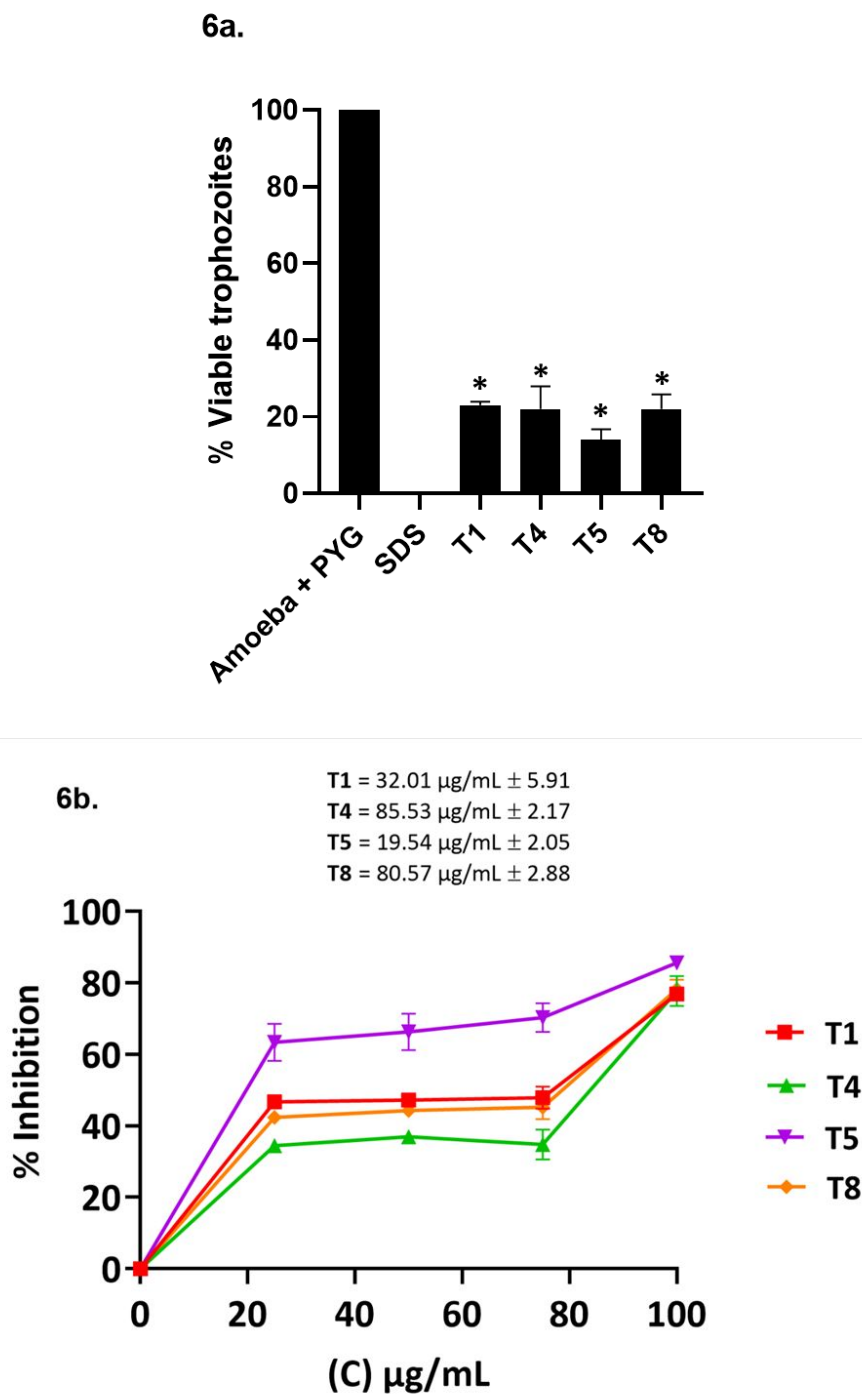


**Figure 6.** Excystation activity of selected compounds against *A. castellanii*. The compounds significantly inhibited excystation process in amoeba. (A) Represents the excystation potential of compounds at 100  $\mu\text{g/mL}$  whereas. (B) Half-minimal inhibitory concentration. The data presented the mean  $\pm$  standard error of three independent trails performed in duplicates.

***Compounds showed minimal cytotoxicity but failed to protect amoebae mediated human cell death***

Compounds (**T1**, **T4**, **T5** and **T8**) were evaluated for their toxicity against HCT-116 cells. The LDH assays revealed that all these compounds exhibited limited cytotoxicity against human cells at a concentration of 100  $\mu\text{g/mL}$  (**Figure 7**). Out of all these compounds, **T1** that showed the highest excystation activity showed the least cytotoxic effects of 17% at concentration that 5-fold its excystation  $\text{MIC}_{50}$  concentration whereas **T5** and **T8** showed 35% cytopathic properties against human cells (**Figure 7**). When the amoebae were pre-treated with these compounds, they failed to protect the pathogen mediated human cell cytotoxicity (**Figure 8**).

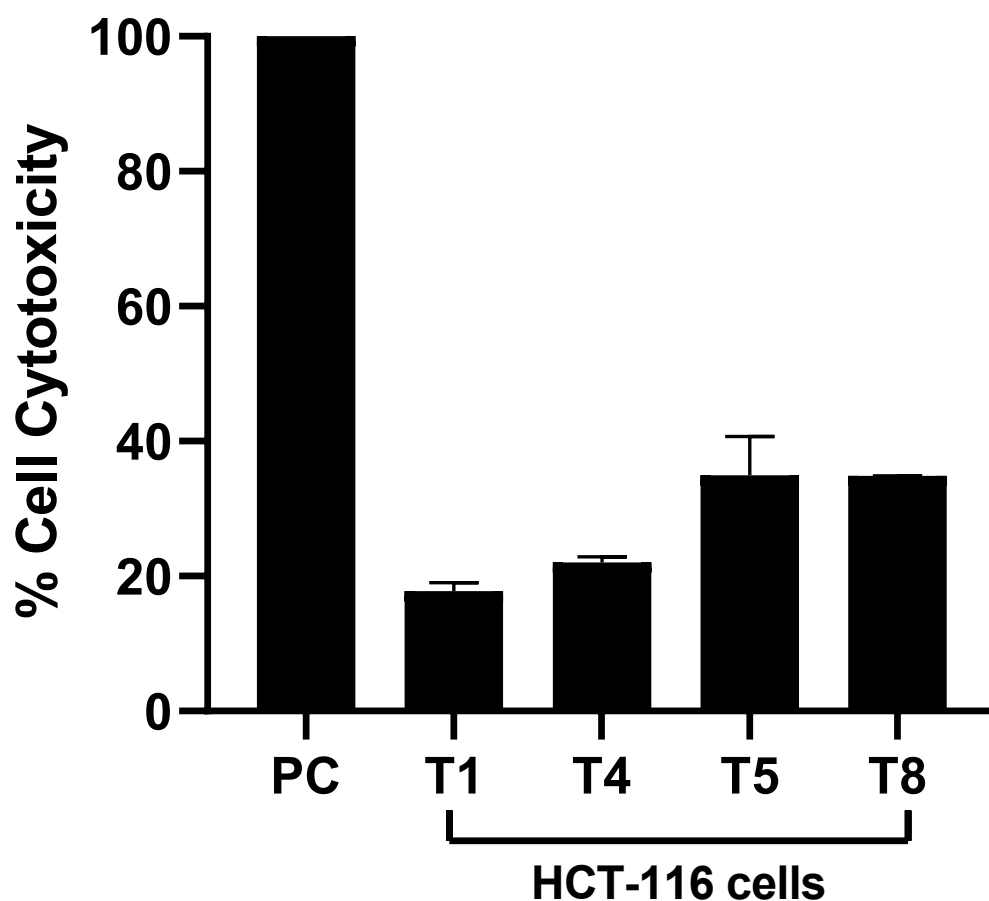


**Figure 7. Cytotoxic activity.** All the compounds showed minimal cytotoxicity against human cells.

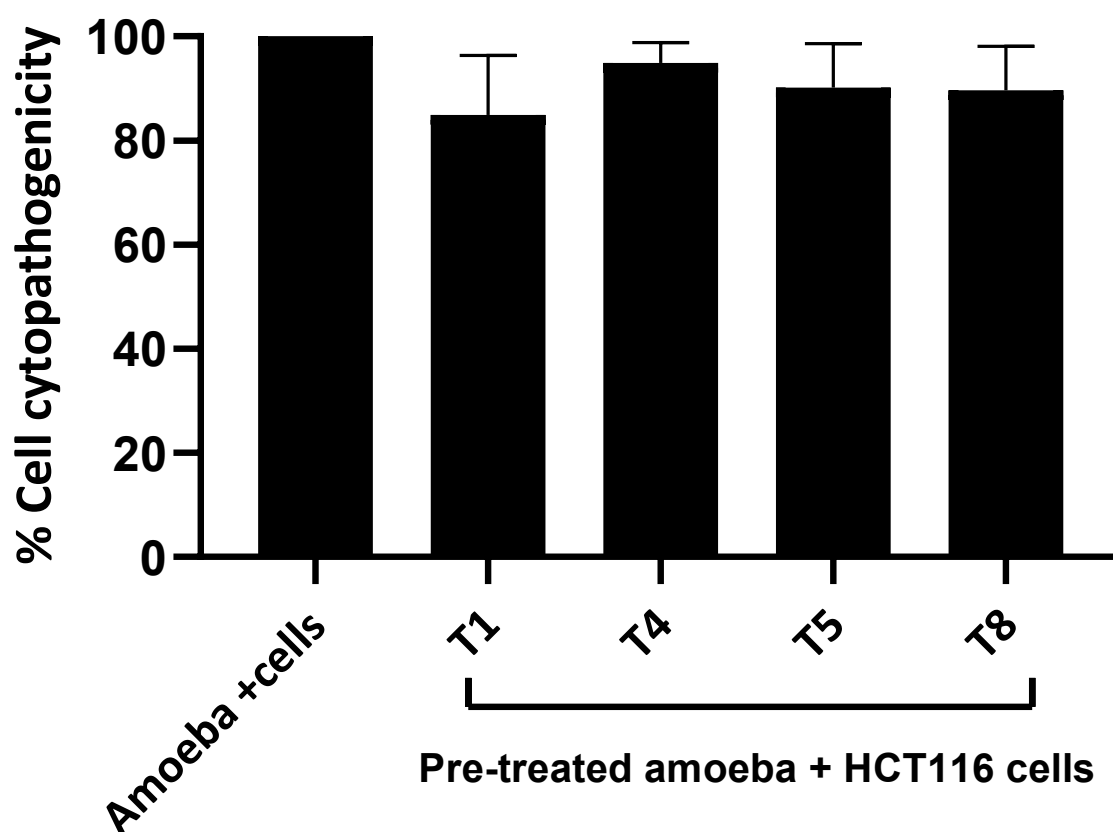


**Figure 8. Pre-treatment of amoeba with compounds did not defend human cell death.** All the experiments were performed three time in duplicates and the data presented as the mean  $\pm$  standard error of three independent trails done in duplicates.

***Molecular docking showed superior binding efficacy of compound T5 in Acanthamoeba CYP51***

Molecular docking study was conducted against *Acanthamoeba* CYP51 using compounds **T1**, **T4**, **T5** and **T8** which showed the most effective antiamoebic effects and excystation inhibitory effects. Compound **T1** emerged as a standout, forming the most stable complex within the *Acanthamoeba* CYP51 active site (PDB: 6UX0). **T1** phenyl ring demonstrated pi-pi stacking interaction with the Phe-116 amino acid residue, while its triazole ring engaged similarly with Tyr-114. Additionally, an aromatic H-bond interaction was observed between **T1** phenyl ring and Ala-290. The compound also showed multiple hydrophobic interactions

with Hem-501, Tyr-114, Leu-363, Phe-365, Leu-364, Val-126, Ala-294, and Tyr-114, significantly stabilizing the ligand-receptor complex (**Figure 9A, Table 1**).

**T4** triazole ring displayed a H-bond interaction with Leu-364, while its phenyl rings engage in pi-pi interactions with phe-116. Multiple hydrophobic interactions were observed between **T4** and amino acid residues, including Met-367, Leu-363, HEM-501, Val-366, Val-221, Phe-116, Tyr-114, Met-367, Tyr-468 and Tyr-127 (**Figure 9B, Table 1**). In contrast, compound **T5** exhibited less interaction with the binding site, primarily involving pi-pi stacking with Tyr-127 and hydrophobic interactions with Val-126, Ala-290, Leu-138, Leu-291, Ile-141, Phe-121, Phe-116, Phe-293, Ser-390, Phe-365, and Met-367 (**Figure 9C, Table 1**). However, **T8** reveals several interactions with various amino acid residues within the *Acanthamoeba* CYP51 active site (PDB: 6UX0). The phenyl ring of **T8** forms pi-pi interactions with Phe-116, chlorine atom form halogen bond with Ser-117, while phenyl ring forms aromatic H-bonds with Tyr-137, phenylalanine 116, and serine 117. Additionally, a halogen bond is observed with tyrosine 127. It exhibited several hydrophobic interactions with Thr-298, Leu-363, Ala-294, Gly-295, HEM-501, Tyr-114, Phe-116, Ala-290, Phe-365, Val-221, Met-367, and Tyr-127 (**Figure 9D, Table 1**). Therefore, the findings highlight the potential of compounds **T4**, **T5** and **T8** as promising candidates for further development in combating *Acanthamoeba* infections by targeting CYP51.

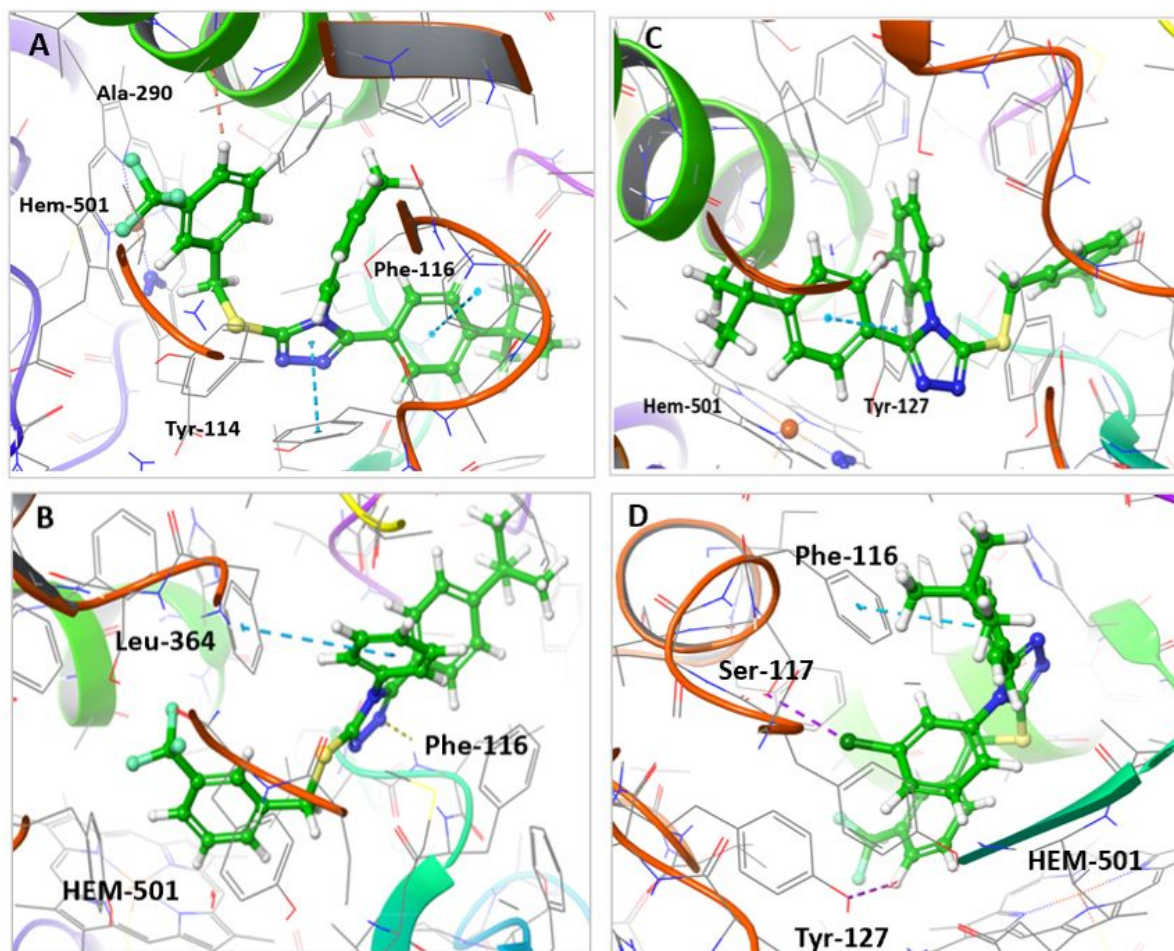


**Figure 9.** Molecular docking of compounds within the active site of *Acanthamoeba* CYP51 enzyme (PDB:6UX0). (A) T1. (B) T4. (C) T5. (D) T8.

**Table 1.** Molecular modeling of the most active compounds T1, T4, T5 and T8 within the *Acanthamoeba* CYP51 binding active site (PDB: 6UX0).

Compound	Moiety	Interaction	Amino acid
T1	Triazole ring	Pi-pi interaction	Tyr-114
	Phenyl ring	Aromatic H-bond	Ala-290
	Phenyl ring	Pi-pi interaction	Phe-116
	Sulfanyl	Hydrophobic interaction	HEM-501
	Phenyl	Hydrophobic interaction	Ala-294, Phe-293
	<i>tert</i> -butyl	Hydrophobic interaction	Leu-364, Phe-365

	Triazole ring	Hydrophobic interaction	Tyr-114, Tyr-127, Leu- 363
	CF <sub>3</sub>	Hydrophobic interaction	HEM-501, Val-126
<b>T4</b>	Triazole ring	H-bond interaction	Leu-364
	Phenyl ring	Pi-pi interaction	Phe-116
	Phenyl ring	Hydrophobic interaction	Met-367, Leu-363, HEM-501, Val-366, Val-221, Phe-116
	Sulfanyl	Hydrophobic interaction	Phe-116, Tyr-114, Met-367
	<i>tert</i> -butyl	Hydrophobic interaction	Tyr-468
	CF <sub>3</sub>	Hydrophobic interaction	Tyr-127
<b>T5</b>	Phenyl ring	Pi-pi interaction	Tyr-127
	<i>tert</i> -butyl	Hydrophobic interaction	Ala-290, Leu-138
	Phenyl ring	Hydrophobic interaction	Val-126, Leu-291, Ile-141
	CF <sub>3</sub>	Hydrophobic interaction	Ser-390
	Triazole ring	Hydrophobic interaction	Phe-365, Met-367, HEM-501, Phe-116, Phe-12
<b>T8</b>	Phenyl ring	Pi-pi interaction	Tyr-137
	Phenyl ring	Aromatic H-bond	Phe-116
	Cl	Halogen bond	Ser-117
	Sulfanyl	Hydrophobic interaction	Thr-298, Leu-363, Ala-294, Gly29
	Phenyl	Hydrophobic interaction	HEM-501, Tyr-114, Phe-116
	<i>tert</i> -butyl	Hydrophobic interaction	Phe-365, Phe-116, Val-221, Met-367
	CF <sub>3</sub>	Hydrophobic interaction	HEM-501, Ala-290
	Cl	Hydrophobic interaction	Tyr-127

### ***Compounds T1-T10 displayed promising pharmacokinetics characteristics***

Compounds **T1-T10** exhibit promising attributes in terms of molecular weight (MW) and lipophilicity, aligning with the typical requirements for moderate oral bioavailability, as detailed in **Table 2**. T1-T10 compounds are not permeable to the blood-brain barrier (BBB), without showing PAINS (Pan-Assay Interference Compounds) alerts. Topological Polar Surface Area (TPSA) values indicate oral viability. Notably, the bioavailability radar for the

most active candidates, **T1**, **T4**, **T5** and **T8**, demonstrates an optimal range of properties, as illustrated in **Figure 10**.

**Table 2.** ADMET properties of **T1-T10** compounds

Molecule	MW	#Rotatable bonds	#H-bond acceptors	TPSA	iLOGP	BBB permeant	Bioavailability Score	PAINS #alerts
<b>T1</b>	532.42	7	5	56.01	4.52	No	0.17	0
<b>T2</b>	471.51	7	6	56.01	4.32	No	0.55	0
<b>T3</b>	487.97	7	5	56.01	4.35	No	0.55	0
<b>T4</b>	467.55	7	5	56.01	3.97	No	0.55	0
<b>T5</b>	481.58	7	5	56.01	4.47	No	0.55	0
<b>T6</b>	535.55	8	8	56.01	4.48	No	0.17	0
<b>T7</b>	497.58	8	6	65.24	4.23	No	0.55	0
<b>T8</b>	501.99	7	5	56.01	4.52	No	0.17	0
<b>T9</b>	483.55	8	6	65.24	4.39	No	0.55	0
<b>T10</b>	485.54	7	6	56.01	4.43	No	0.55	0

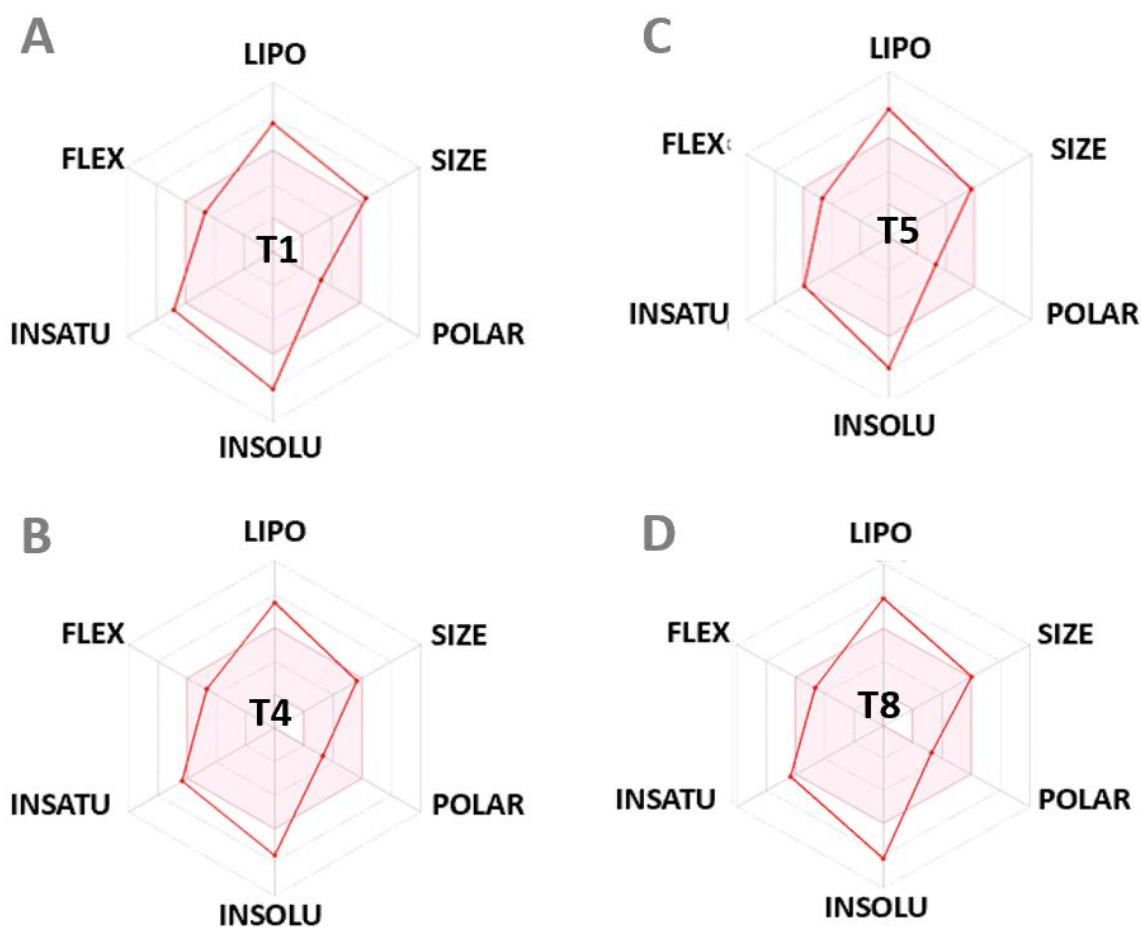


**Figure 10.** Bioavailability radar of (A) T1, (B) T4, (C) T5 and (D) T8. The pink area indicates preferred properties range.

***R-group analysis reveals structural insights driving superior excystation inhibitory activity of T5 compound***

R-group analysis of excystation inhibitory activity of the compounds showed that the best activity of compound T5 with R substitution of *tert*-butyl and R1 substitution of 4-tolyl group followed by T1 with R substitution of iso-propyl and R1 substitution of 3-Br group as indicated in heatmap (Figure 11A). The hydrophobic group at R1 significantly reduced the activity, while in R2 and R3 significantly increased the activity. The hydrogen bond acceptor significantly increased the activity (Figure 11B). This may explain the superior activity of T5 compound.

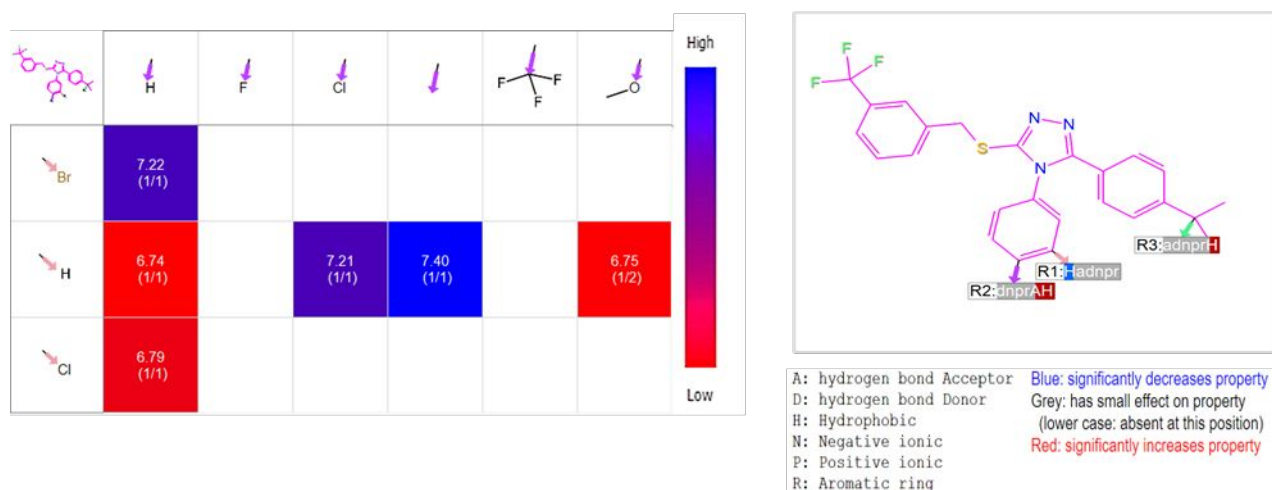


**Figure 11.** SAR Heatmap evaluation. (A) PIC<sub>50</sub> excystation values were depicted as colors ranging from red to blue. (B) Pharmacophoric QSAR analysis. Red, grey, and blue hues were exhibited as characteristics key.

## Discussion

Free-living parasites called *Acanthamoeba* are prevalent and capable of infecting people and other animals simultaneously in opportunistic and non-opportunistic strategies<sup>17</sup>. The

parasite coexists in both trophozoites and the hardy cysts forms. The cysts is the dormant stage and can withstand the harsh conditions<sup>18</sup>. In the trophozoite stages, the amoeba causes rare but fatal infections of the eye and central nervous system (CNS), Granulomatous amoebic encephalitis (GAE) and *Acanthamoeba* keratitis, respectively in immunocompetent individuals<sup>17-19</sup>. Amoebiasis is difficult to manage, and chances of recovery can be depressing, particularly in severe instances. To increase the probability of a favourable outcome, early diagnosis and immediate management are essential<sup>20-22</sup>.

The reported efficacy of azole compounds in combating *Acanthamoeba* infections was highlighted in various studies. Azoles as metronidazole, itraconazole, fluconazole, and their derivatives have demonstrated significant anti-amoebic activity, and as potential treatment options for these parasitic infections<sup>23,24</sup>. Metronidazole, for example, has been widely recognized for its effectiveness against *Acanthamoeba*, causing DNA breakdown through apoptosis-like processes in *Blastocystis Anthropos*<sup>25</sup>. Additionally, the conjugated metronidazole showed remarkable antiamoebic efficacy against *Entamoeba histolytica*, with reduced cytotoxicity for human cells<sup>26</sup>. Tinidazole and ornidazole have also shown substantial antiamoebic properties comparable to that of metronidazole<sup>27,28</sup>. Tinidazole, in particular, has been successfully used to treat *Entamoeba histolytica*-mediated amoebic liver abscess with a single dose<sup>29</sup> and has been applied in the management of *Trichomonas* species that are resistant to metronidazole<sup>30</sup>. Furthermore, the effectiveness of triazole CYP51 inhibitors such as fluconazole, itraconazole, and voriconazole were studied against *Acanthamoeba castellanii* and *Acanthamoeba polyphaga* infections in humans. Itraconazole and voriconazole showed stronger binding and inhibition of CYP51 activity in *A. castellanii*, than fluconazole. However, itraconazole was less effective than voriconazole, in inhibiting *Acanthamoeba* cell division and fluconazole did not hinder cell growth. Voriconazole emerged as a promising inhibitor of trophozoite proliferation for both *A. castellanii* and *A. polyphaga*, suggesting its potential for controlling *Acanthamoeba* infections in comparison to itraconazole<sup>31</sup>.

Collectively, these suggest that selected azole derivatives hold promise as potential antiamoebic drugs<sup>32</sup>. Their ability to exhibit amoebicidal efficacy at microgram dosages underscores their significance in managing parasitic infections. Furthermore, the observation that these compounds remarkably block the excystation mechanisms in *Acanthamoeba* highlights their potential in preventing the transition of the parasite from its dormant cyst form to the active trophozoite form, which is a critical aspect of controlling *Acanthamoeba*

infections. Azoles such as isavuconazole targeting sterol 14-demethylase (CYP51), have also demonstrated high potency against amoebic diseases. Isavuconazole is considered an affordable choice for treating both primary and recurring *Acanthamoeba keratitis* (AK) due to its safety profile and its capacity to inhibit *Acanthamoeba castellanii's* excystation mechanism<sup>33</sup>.

In the present study, we designed and synthesized a series of thiazole scaffold-based compounds that previously showed antifungal activity against *Candida*<sup>34</sup> and were tested in the current study on *Acanthamoeba*. Amoebicidal assays revealed that selected compounds indicated important antiamoebic activity at concentration 100 µg/mL. Compounds **T1** and **T8** exhibited significant amoebicidal effects, reduced amoeba viability, and displayed lowest MIC<sub>50</sub> values. Notably, compounds **T5**, **T3**, and **T1** displayed remarkable anti-excystation activity. The results sheds light on the potential of azole compounds, particularly **T1** and **T5**, as promising anti-*Acanthamoeba* agents that demonstrate both amoebicidal and anti-excystation activities, while maintaining low cytotoxicity to human cells.

The optimal molecular properties of compounds **T1** and **T5** suggest the potential for moderate oral bioavailability. The R-group analysis reveals that specific R-group substitutions play a pivotal role in enhancing the inhibitory activity against excystation in *Acanthamoeba*. Notably, **T5**, with its *tert*-butyl and 4-tolyl substitutions at R and R1 positions, respectively, emerged as the most effective compound in preventing excystation. On the other hand, the *tert*-butyl group of **T4** and **T8** and the chlorine substitution of **T8** responsible for their activity. Additionally, **T1** displayed noteworthy activity, driven by its iso-propyl and 3-Br substitutions at R and R1 positions. This finding is crucial as inhibiting excystation can help maintain the amoeba in its latent cyst form, rendering it more susceptible to immune system attack.

Compound **T5** stands out with its low MIC<sub>50</sub> value for excystation inhibition and limited cytotoxicity to human cells at 5-fold its MIC<sub>50</sub> value that ensured safety profile. Molecular docking studies provide insights into the potential binding interactions of compounds within the *Acanthamoeba* CYP51 active site. Compound **T5** shows superior binding interactions, including pi-pi stacking and hydrophobic interactions, suggesting its efficacy as a targeted treatment.

Concluded, the collective evidence suggests that azole compounds especially triazoles have the potential to be effective antiamoebic agents. Further mechanistic research and clinical

studies are needed to validate their efficacy and safety for therapeutic use against *Acanthamoeba* infections, both as primary treatment options and in cases of recurrence. These findings contribute to the ongoing efforts to combat these parasitic infections effectively.

## Experimental

### Chemistry

Chemicals and solvents are of analytical grade and were purified and dried using standard techniques. Thin-layer chromatography (TLC) was used to monitor reactions using pre-coated silica gel plates (kiesel gel 60 F254, BDH), and spots were observed under UV light (254nm). The melting points were determined without correction using Gallenkamp melting point equipment (Staffordshire, UK). A Bruker spectrometer was used to record <sup>1</sup>HNMR and <sup>13</sup>CNMR spectra at 500 MHz. The signals were denoted as follows: s, singlet; d, doublet; t, triplet; m, multiplet. Chemical shifts were indicated in parts per million (ppm) relative to tetramethylsilane and coupling constant (J) values were represented in hertz (Hz).

Electrospray ionization (ESI) mass spectrum was used to obtain mass spectroscopic data.

### ***Summarized multistep synthetic procedure of the T1-T10 compounds***

The synthesis was performed according to our previous publication <sup>34</sup>. The process involved the reaction of the acid hydrazides with substituted phenyl isothiocyanates in ethanol to synthesize 4-substituted benzoyl-*N*-substituted phenyl thiosemicarbazides. The synthesis of triazole thiol involved refluxing thiosemicarbazides in 2N NaOH, followed by neutralization with an HCl solution. Subsequent reaction of the triazole thiol with 3-trifluoro benzyl chloride in ethanol yielded the corresponding *S*-alkylation triazole thiol compounds **T1-T10**.

Detailed synthesis of the compounds is summarized in **Supplementary Data**.

### Biology

### ***Culturing HCT-116 cell line***

Human colon cancer cell lines were purchased from the American type culture collection (ATCC) and normally grown in Roswell Park Memorial Institute (RPMI) supplemented with 10% fetal bovine serum (FBS), 1% minimum essential medium nonessential amino acid (MEM NEAA), 10% nu-serum, 1% penicillin-streptomycin, and 1% L-glutamine at 37°C in the presence of 5% CO<sub>2</sub> and 95% humidity. Upon 80-90% confluency, the monolayer was trypsinized with 2 mL of trypsin for 5 min at 37 °C. Approximately 10,000 cell/well was seeded in each well of a 96-well plate. The plate was then incubated for 24-48 h at 37 °C in an incubator containing 5% CO<sub>2</sub> and 95% humidity. The monolayer was established and was used in cell based assays <sup>47, 48</sup>.

### ***Acanthamoeba cultures***

*A. castellanii* genotype T4 (ATCC 50492) was cultured in 10 mL protease-peptone yeast glucose (PYG) medium (yeast extract 0.75 %(w/v), proteose peptone 0.75 %(w/v) and glucose 1.5 % (w/v)) at 30°C in 75 cm<sup>3</sup> tissue culture flasks as previously reported <sup>49</sup>. The surface-adherent trophozoites of *A. castellanii* were dislodged by incubating the flasks on ice for 20 min followed by gentle tapping to detach the amoebae. The suspension was thereafter collected in a 50 mL falcon tube and centrifuged at 3000 g for 5 min. The amoeba pellet was re-suspended in 1 mL of RPMI, counted using a haemocytometer, and then utilized in further tests <sup>50, 51</sup>.

### ***Amoebicidal assays***

The antiamoebic effects of compounds (**T 1-10**) were evaluated using amoebicidal assays, as described previously <sup>50</sup>. Briefly, in 24-well plates, 5 x10<sup>5</sup> *A. castellanii* trophozoites were incubated with 100 µg/mL of all the tested compounds for 24 h at 30°C. For positive control, 25 µM chlorhexidine was used, whereas negative controls consisted of amoeba alone. Additionally, dimethyl sulfoxide (DMSO) was used as solvent control. Following 24-h incubation at 30 °C, a trypan blue exclusion test was performed to determine the estimated average viable amoebae count for each treatment. In some experiments, compounds with significant amoebicidal effects were evaluated at different concentrations (25 µg/mL, 50 µg/mL, 100 µg/mL, 200 µg/mL and 400 µg/mL) to conclude their half minimum inhibitory concentration (MIC<sub>50</sub>) <sup>23</sup>.

### ***Encystation assays***

The selected compounds were evaluated for their anti-amoebic effects using encystation assays<sup>52</sup>. Initially,  $1 \times 10^6$  amoeba trophozoites were cultured for 48 h at 30 °C with 100 µg/mL of the compounds in the presence of 16 % filter-sterilized glucose as encystation medium. Next, 0.1% sodium dodecyl sulphate (SDS) was added to each well of the 24-well plate, which was then agitated for 10-15 min. The remaining cysts were counted using a haemocytometer, and the results were recorded. As a control, *A. castellanii* was grown alone in 16% glucose<sup>48</sup>.

### ***Excystation assays***

*A. castellanii* cysts were produced by culturing amoeba trophozoites in phosphate-buffered saline (PBS) on non-nutrient bacteriological agar plates at 30°C for two weeks. PBS was added to non-nutrient agar plates containing amoeba cysts, and the amoeba cysts were scraped off the plates. Amoeba culture was centrifuged at 3000 g for 5 min and the pellet was resuspended in serum-free RPMI to adjust the starting culture for the encystation tests. To evaluate the excystation process,  $2 \times 10^5$  *A. castellanii* cysts were cultured with 100µg/mL of selected compounds in a final volume of 500 µL of PYG medium. As a control, amoeba cysts produced in PYG alone were used. The plates were incubated at 30 °C for 24–72 h, while they were regularly monitored. Then, the viable amoeba trophozoites were counted and recorded using a haemocytometer<sup>53</sup>. For half-minimum inhibitory effects, these compounds were tested at different concentrations (*i.e.*, 25 µg/mL, 50 µg/mL, 75 µg/ mL and 100 µg/mL) and results were recorded.

### ***Cytotoxicity assays***

To evaluate the *in vitro* cell cytotoxicity of (**T 1-10**) compounds utilizing human cells, lactate dehydrogenase (LDH) experiments were conducted<sup>47, 48</sup>. In a 96-well plate, the monolayer of HCT-116 cells was exposed to 100 µg/mL of these compounds. After this, the plate was incubated for 24 h at 37°C, with 95% humidity and 5 % CO<sub>2</sub>. For positive control, the plate was incubated at 37°C for 45 min with triton X-100 (0.1%). Following that, an equivalent volume of LDH kit reagents was combined with an equal volume of cell supernatant containing liberated LDH enzyme to assess the LDH released in the following equation:

$$\% \text{ Cytotoxicity} = \frac{\text{sample value} - \text{negative control value}}{\text{positive control value} - \text{negative control value}} \times 100$$

For positive and negative controls, cell monolayers were treated with 0.1%Triton X-100 and RPMI alone, respectively.

### ***Cytopathogenicity assays***

Cytopathogenicity assays were performed to determine the amoeba-mediated host cell death. Firstly,  $2 \times 10^5$  *A. castellanii* trophozoites were treated with selected compounds at a concentration of 100  $\mu\text{g/mL}$  for 2 h at 30°C. After this incubation, the culture containing amoeba was centrifuged at 3000 g for 5 min and the pre-treated amoebae were re-suspended in RPMI. The RPMI containing the pre-treated amoeba were added to each well of 96-well plate with established cell monolayer<sup>54</sup>. The plate was incubated at 37°C for 24 h with 5% CO<sub>2</sub> and 95% humidity. Positive and negative controls were generated in quadruplicate by treating HCT-116 cells with 1% Triton X-100 (100 percent cell death) and amoebae in RPMI alone, respectively. After 24 h of incubation, each well's supernatant was equally combined with the enzyme lactate dehydrogenase (LDH) assays kit reagents and assessed amoebae mediated cytotoxicity at 490 nm.

### **Computational study**

All computational studies were conducted utilizing Schrödinger Suite 12.7, which is accessible at [www.Schrödinger.com](http://www.Schrödinger.com). Maestro graphical user interface software was employed.

### ***Protein preparation***

The 3D crystal structures of isavuconazole bounded to *Acanthamoeba castellanii* CYP51(PDB: 6UX0) enzyme was downloaded from the protein data bank available at (<https://www.rcsb.org/>). The proteins were prepared and refined using the Protein Preparation Wizard<sup>35</sup>. Crystallography of water molecules beyond 5Å were removed. All the missing hydrogen atoms were added at pH 7.5 for appropriate ionization and the tautomerization state of amino acid residues and proper bond order were assigned. Subsequently, the refining of protein structures was performed and the water molecules with < 3 hydrogen bonds to non-waters were deleted. Finally, the energy minimization was done using OPLS-4 to relieve the steric clashes<sup>36</sup>.

### ***Ligand preparation***

The 2D structures of the design compounds were converted to 3D structures using LigPrep, Schrodinger<sup>37</sup>. Hydrogen atoms were added, and the salt ions were removed. The most probable ionization states were calculated at pH 7.5 using the Epik module<sup>38,39</sup>. During the ligand preparation, specified chirality of the 3D crystal structure was retained. The subsequent energy minimization of each structure was carried out using OPLS4 force field<sup>36</sup> and filtered through a relative energy tool. Besides, any errors in the ligands were eradicated in order to enhance the accuracy of the molecular docking<sup>40</sup>.

### ***Grid generation***

The isavuconazole ligand in crystal structure of bound complex of *Acanthamoeba castellanii* CYP51 was used for grid generation. A grid box was generated at the centroid of the active site for subsequent docking studies, defining the active site based on the ligand's crystal structure.

### ***Molecular docking***

Molecular docking was performed within the catalytic pocket site of the proteins using standard precision (SP) mode of Grid using Glide<sup>41,42</sup>. The prepared ligands were docked against grid generated *Acanthamoeba castellanii* CYP51 (PDB: 6UX0) in SP flexible mode<sup>43</sup>.

### ***ADMET predication***

The selected compounds were undergone computational ADMET analysis to identify those with best absorption, distribution, metabolism, elimination, and toxicity profiles. Achieving optimal bioavailability is dependent on a balanced combination of solubility and partitioning characteristics. Total polar surface area (TPSA) and the number of rotatable bonds are essential absorption and bioavailability parameters using the Swiss-ADME server [30]. Furthermore, the new compounds were evaluated for compliance with Lipinski's Rule of Five

in order to identify their suitability as innovative pharmaceutical candidates<sup>44</sup>. The Swiss-ADME service was used to analyse them<sup>45</sup>.

### ***R-group analysis***

R-group mapping analysis was conducted using the Schrödinger suite. Initially, the input prepared 3D-structure, along with its MIC<sub>50</sub> values, was transformed into PIC<sub>50</sub> values. The process involved common core identification by employing Combi-Glide for bond labelling and structural alignment that focused on the fingerprint similarity of the sidechain to minimize the number of attached R-groups. The results of this analysis were visualized as a heatmap, using distinct color gradients, reflecting their respective PIC<sub>50</sub> values. Furthermore, QSAR model was developed based on pharmacophoric features, encompassing hydrophobic group (H), hydrogen bond donor (D), acceptor (A), negatively ionizable (N), positively ionizable (P), and aromatic ring (R)<sup>46</sup>.

### **Statistical analysis**

The data analysis and representations were performed using GraphPad Prism version 8.0.2 (GraphPad Software; San Diego, CA, USA). All the treatments and associated controls were compared using the two-sample, two-tailed t-test. The data are represented as the mean of three replicates.

### **Authors' contributions**

**Conceptualization:** BQ, NK and SSMS. **Data curation:** BQ, RH, NA, NK, and SSMS. **Formal analysis:** BQ and SSMS. **Funding acquisition:** BQ, and SSMS. **Investigation:** RH, NA and SSMS. **Methodology:** BQ, RH, and NA. **Supervision:** BQ, NK, and SSMS. **Writing-original draft:** BQ, RH, NA, and SSMS. **Writing-review & editing:** BQ, RH, NA, NK and SSMS. All authors approved the submitted version.

## Acknowledgements

The authors acknowledge the generous funding from the University of Sharjah (Grant# 2101090286) to BQ and SSMS, and by the support from the Air Force Office of Scientific Research (AFOSR), USA to NK.

## Conflict of interest

The authors declare no conflicts of interest.

## Supplementary data

Detailed synthesis of the compounds and analysis are indicated in **Supplementary Data**.

## Reference

1. G. S. Visvesvara, H. Moura and F. L. Schuster, *FEMS Immunology & Medical Microbiology*, 2007, **50**, 1-26.
2. R. Siddiqui, N. A. J. P. Khan and vectors, 2012, **5**, 1-13.
3. Y. Wang, L. Jiang, Y. Zhao, X. Ju, L. Wang, L. Jin, R. D. Fine and M. J. F. i. M. Li, 2023, **14**, 1147077.
4. F. Marciano-Cabral and G. J. C. m. r. Cabral, 2003, **16**, 273-307.
5. C. Bunsuwansakul, T. Mahboob, K. Hounkong, S. Laohaprapanon, S. Chitapornpan, S. Jawjit, A. Yasiri, S. Barusrux, K. Bunluepuech and N. J. T. K. j. o. p. Sawangjaroen, 2019, **57**, 341.
6. R. Abdul Halim, R. H. Mohd Hussain, S. Aazmi, H. Halim, N. Ahmed Khan, R. Siddiqui, T. J. J. o. W. Shahrul Anuar and Health, 2023, **21**, 1342-1356.
7. F. L. Schuster and G. S. J. D. R. U. Visvesvara, 2004, **7**, 41-51.
8. S. M. Siddiqui, A. Salahuddin and A. J. E. j. o. m. c. Azam, 2012, **49**, 411-416.
9. M. A. Farha and E. D. Brown, *Nature microbiology*, 2019, **4**, 565-577.
10. S.-M. Lee, M.-S. Kim, F. Hayat and D. Shin, *Molecules*, 2019, **24**, 3886.
11. W. Zhou, A. G. Warrilow, C. D. Thomas, E. Ramos, J. E. Parker, C. L. Price, B. H. Vanderloop, P. M. Fisher, M. D. Loftis and D. E. Kelly, *Biochimica et Biophysica Acta (BBA)-Molecular and Cell Biology of Lipids*, 2018, **1863**, 1164-1178.
12. B. Negi, P. Poonan, M. F. Ansari, D. Kumar, S. Aggarwal, R. Singh, A. Azam and D. S. Rawat, *European Journal of Medicinal Chemistry*, 2018, **150**, 633-641.
13. B. Rasmussen, K. Bush and F. Tally, *Clinical Infectious Diseases*, 1997, **24**, S110-S120.
14. P. Upcroft and J. A. Upcroft, *Clinical microbiology reviews*, 2001, **14**, 150-164.
15. M. Andrzejewska, L. Yépez-Mulia, R. Cedillo-Rivera, A. Tapia, L. Vilpo, J. Vilpo and Z. Kazimierczuk, *European journal of medicinal chemistry*, 2002, **37**, 973-978.
16. D. Hernández-Martínez, M. Reyes-Batlle, I. Castelan-Ramírez, P. Hernández-Olmos, V. Vanzzini-Zago, E. Ramírez-Flores, I. Sifaoui, J. E. Piñero, J. Lorenzo-Morales and M. Omaña-Molina, *Experimental parasitology*, 2019, **197**, 29-35.

17. G. S. J. H. o. c. n. Visvesvara, 2013, **114**, 153-168.
18. N. A. J. F. m. r. Khan, 2006, **30**, 564-595.
19. J. Lorenzo-Morales, N. A. Khan and J. J. P. Walochnik, 2015, **22**.
20. S. C. Parija, K. Dinoop and H. J. T. P. Venugopal, 2015, **5**, 23.
21. G. Varacalli, A. Di Zazzo, T. Mori, T. H. Dohlman, S. Spelta, M. Coassin and S. J. J. o. c. m. Bonini, 2021, **10**, 942.
22. N. Fanselow, N. Sirajuddin, X.-T. Yin, A. J. Huang and P. M. J. P. Stuart, 2021, **10**, 323.
23. N. Akbar, K. Hussain, M. Khalid, R. Siddiqui, M. R. Shah and N. A. J. J. o. A. M. Khan, 2023, **134**, Ixad072.
24. A. Anwar, M. R. Mungroo, S. Khan, I. Fatima, R. Rafique, Kanwal, K. M. Khan, R. Siddiqui and N. A. J. A. Khan, 2020, **9**, 188.
25. A. Nasirudeen, Y. E. Hian, M. Singh and K. S. J. M. Tan, 2004, **150**, 33-43.
26. A. Salahuddin, S. M. Agarwal, F. AVECILLA, A. J. B. Azam and m. c. letters, 2012, **22**, 5694-5699.
27. G. J. Frayha, J. Smyth, J. G. Gobert and J. J. G. P. T. V. S. Savel, 1997, **28**, 273-299.
28. S. L. J. T. I. Stanley, 2003, **361**, 1025-1034.
29. M. Quaderi, M. S. Rahman, A. Rahman, N. J. T. J. o. T. M. Islam and Hygiene, 1978, **81**, 16-19.
30. L. O. J. N. E. j. o. m. Eckert, 2006, **355**, 1244-1252.
31. D. C. Lamb, A. G. Warrilow, N. J. Rolley, J. E. Parker, W. D. Nes, S. N. Smith, D. E. Kelly and S. L. Kelly, *Antimicrobial Agents and Chemotherapy*, 2015, **59**, 4707-4713.
32. N. M. Mackey-Lawrence and W. A. J. B. C. E. Petri Jr, 2011, **2011**.
33. B. Shing, S. Singh, L. M. Podust, J. H. McKerrow, A. J. A. a. Debnath and chemotherapy, 2020, **64**, 10.1128/aac. 02223-02219.
34. R. Hamdy, B. Fayed, A. M. Hamoda, M. Rawas-Qalaji, M. Haider and S. S. Soliman, *Molecules*, 2020, **25**, 1463.
35. G. M. Sastry, M. Adzhigirey, T. Day, R. Annabhimoju and W. Sherman, *Journal of computer-aided molecular design*, 2013, **27**, 221-234.
36. E. Harder, W. Damm, J. Maple, C. Wu, M. Reboul, J. Y. Xiang, L. Wang, D. Lupyan, M. K. Dahlgren and J. L. Knight, *Journal of chemical theory and computation*, 2016, **12**, 281-296.
37. S. F. Giardina, D. S. Werner, M. Pingle, P. B. Feinberg, K. W. Foreman, D. E. Bergstrom, L. D. Arnold and F. Barany, *Journal of medicinal chemistry*, 2020, **63**, 3004-3027.
38. J. C. Shelley, A. Cholleti, L. L. Frye, J. R. Greenwood, M. R. Timlin and M. Uchimaya, *Journal of computer-aided molecular design*, 2007, **21**, 681-691.
39. J. R. Greenwood, D. Calkins, A. P. Sullivan and J. C. Shelley, *Journal of computer-aided molecular design*, 2010, **24**, 591-604.
40. S. A. Ganai, E. Abdullah, R. Rashid and M. Altaf, *Frontiers in molecular neuroscience*, 2017, **10**, 357.
41. T. A. Halgren, R. B. Murphy, R. A. Friesner, H. S. Beard, L. L. Frye, W. T. Pollard and J. L. Banks, *Journal of medicinal chemistry*, 2004, **47**, 1750-1759.
42. R. A. Friesner, J. L. Banks, R. B. Murphy, T. A. Halgren, J. J. Klicic, D. T. Mainz, M. P. Repasky, E. H. Knoll, M. Shelley and J. K. Perry, *Journal of medicinal chemistry*, 2004, **47**, 1739-1749.
43. R. A. Friesner, R. B. Murphy, M. P. Repasky, L. L. Frye, J. R. Greenwood, T. A. Halgren, P. C. Sanschagrin and D. T. Mainz, *Journal of medicinal chemistry*, 2006, **49**, 6177-6196.
44. A. Daina, O. Michielin and V. Zoete, *Scientific reports*, 2017, **7**, 42717.
45. S. F. Giardina, D. S. Werner, M. Pingle, P. B. Feinberg, K. W. Foreman, D. E. Bergstrom, L. D. Arnold and F. J. J. o. M. C. Barany, 2020, **63**, 3004-3027.
46. R. Hamdy, A. T. Jones, M. El-Sadek, A. M. Hamoda, S. B. Shakartalla, Z. M. Al Shareef, S. S. Soliman and A. D. Westwell, *International Journal of Molecular Sciences*, 2021, **22**, 12272.
47. N. Akbar, R. Siddiqui, M. Iqbal, K. Sagathevan, K. S. Kim, F. Habib and N. A. Khan, *ACS omega*, 2021, **6**, 12261-12273.
48. A. Anwar, A. Soomaroo, A. Anwar, R. Siddiqui and N. A. Khan, *Experimental parasitology*, 2020, **215**, 107915.

49. J. Sissons, K. S. Kim, M. Stins, S. Jayasekera, S. Alsam and N. A. Khan, *Infection and immunity*, 2005, **73**, 2704-2708.
50. N. Akbar, M. I. El-Gamal, B. Q. Saeed, C.-H. Oh, M. S. Abdel-Maksoud, N. A. Khan, A. M. Alharbi, H. Alfahemi and R. Siddiqui, *Antibiotics*, 2022, **11**, 1183.
51. N. A. Khan, E. L. Jarroll, N. Panjwani, Z. Cao and T. A. Paget, *Journal of clinical microbiology*, 2000, **38**, 2858-2861.
52. N. Akbar, R. Siddiqui, M. Khamis, T. Ibrahim, N. A. J. E. Khan and C. Lens, 2021, **47**, 592-597.
53. B. Q. Saeed, K. Hussain, N. Akbar, H. Khan, R. Siddiqui, R. M. Shah and N. A. Khan, *Molecular and Biochemical Parasitology*, 2022, **247**, 111430.
54. R. Siddiqui, N. Akbar, B. Khatoon, M. Kawish, M. S. Ali, M. R. Shah and N. A. J. A. Khan, 2022, **11**, 248.